OPEN ACCESS
IOP PUBLISHING
ENVIRONMENTAL RESEARCH LETTERS
Environ. Res. Lett. **8** (2013) 035014 (7pp)
doi:10.1088/1748-9326/8/3/035014

Permafrost degradation and methane: low risk of biogeochemical climate-warming feedback

Xiang Gao[1], C Adam Schlosser[1], Andrei Sokolov[1], Katey Walter Anthony[2], Qianlai Zhuang[3] and David Kicklighter[4]

[1] Joint Program on the Science and Policy of Global Change, Massachusetts Institute of Technology, Cambridge, MA, USA
[2] Water and Environmental Research Center, University of Alaska, Fairbanks, AK, USA
[3] Departments of Earth and Atmospheric Science, Purdue University, West Lafayette, IN, USA
[4] The Ecosystems Center, Marine Biology Laboratory, Woods Hole, MA, USA

E-mail: xgao304@mit.edu

Received 29 March 2013
Accepted for publication 20 June 2013
Published 10 July 2013
Online at stacks.iop.org/ERL/8/035014

Abstract
Climate change and permafrost thaw have been suggested to increase high latitude methane emissions that could potentially represent a strong feedback to the climate system. Using an integrated earth-system model framework, we examine the degradation of near-surface permafrost, temporal dynamics of inundation (lakes and wetlands) induced by hydro-climatic change, subsequent methane emission, and potential climate feedback. We find that increases in atmospheric CH_4 and its radiative forcing, which result from the thawed, inundated emission sources, are small, particularly when weighed against human emissions. The additional warming, across the range of climate policy and uncertainties in the climate-system response, would be no greater than 0.1 °C by 2100. Further, for this temperature feedback to be doubled (to approximately 0.2 °C) by 2100, at least a 25-fold increase in the methane emission that results from the estimated permafrost degradation would be required. Overall, this biogeochemical global climate-warming feedback is relatively small whether or not humans choose to constrain global emissions.

Keywords: permafrost, methane, climate feedback
S Online supplementary data available from stacks.iop.org/ERL/8/035014/mmedia

1. Introduction

There is general agreement that 21st century warming will be pronounced at higher latitudes. One likely ramification of this warming will be the increased vulnerability of the large carbon reservoirs in the Arctic and boreal permafrost (Schuur and Abbott 2011). Permafrost thaw influences local hydrology, vegetation composition, and ecosystem functioning (Smith *et al* 2005, Christensen *et al* 2004). Of particular concern is the permafrost in near-surface, carbon-rich, ice-rich soils. Increased thawing of these soils can transform the hydrologic landscape to aid in the formation/expansion of saturated areas such as lakes and wetlands (Zimov *et al* 1997, Shindell *et al* 2004). Subsequently, anaerobic decomposition of thawed organic carbon results in emission of methane, a potent greenhouse gas, which could constitute a positive feedback to the climate system (Walter *et al* 2006, Anisimov 2007).

Table 1. Summary of simulation experiments conducted in this study.

TCR	Emission	Notes	Abbreviation
	Unconstrained emission (UCE)		
High (95%)	Median (1330 ppm CO_2 equivalent)	+17 regional patterns	HTCR
Median (50%)		Baseline	MTCR
Low (5%)		+17 regional patterns	LTCR
Median (50%)	High (95%) (1660 ppm CO_2 equivalent)		MTCR_HEM
	Low (5%) (970 ppm CO_2 equivalent)		MTCR_LEM
	Greenhouse gas stabilization (GST)		
High (95%)	Median (560 ppm CO_2 equivalent)	+17 regional patterns	H560
Low (5%)		+17 regional patterns	L560

Despite the importance of the Arctic eco-hydrologic system, considerable uncertainty remains in projections of permafrost degradation and estimates of current high latitude CH_4 flux and future methane emission in response to climate change. Prior studies demonstrate that the extent of near-surface permafrost degradation could differ dramatically as a result of model deficiencies in soil physics and discretizations (Lawrence and Slater 2005, Delisle 2007, Alexeev *et al* 2007, Lawrence *et al* 2008). A comprehensive assessment of CH_4 fluxes that combines inverse modeling with process modeling and flux extrapolation gives a total range of 20–72 $TgCH_4\ yr^{-1}$ for northern regions (EPA 2010). Recent estimates of methane emission increases over the 21st century also vary widely, from 34 to 70 $TgCH_4\ yr^{-1}$ from northern wetlands (Shindell *et al* 2004, Koven *et al* 2011) and from 1.84 (Huissteden *et al* 2011) to 13 $TgCH_4\ yr^{-1}$ (Bastviken *et al* 2011) from the high latitude lakes. Such a wide range of estimates raises questions about how severe methane emission from Arctic permafrost thaw would contribute to future global-scale climate feedbacks (Huissteden *et al* 2011, Delisle 2007, Schuur and Abbott 2011).

Herein we apply an integrated assessment model framework to examine future near-surface permafrost and saturated-area extent as well as the global climate-feedback strength associated with subsequent methane emissions—all bracketed within known sources of uncertainty. Additionally, a model sensitivity analysis is presented that examines the extent to which additional methane emissions provide a more salient (positive) climate-warming feedback (hereinafter a global temperature increase of 0.2 °C is considered a salient feedback). Our study focuses on the methane emission under saturated (anaerobic) soils, thus CO_2 release from thawing soils and its feedback is not included here.

2. Model

The MIT Integrated Global System Model (IGSM) quantifies various sources of uncertainty in climate projections. The IGSM includes sub-models of the natural earth system coupled to a global economic model (The Emission Prediction and Policy Analysis or EPPA) (Sokolov *et al* 2005). The IGSM sub-model of atmospheric dynamics and chemistry is two-dimensional in altitude and latitude coupled to a mixed layer ocean component. The parameterizations of physical processes (convection, radiation, etc) resemble the Goddard Institute for Space Studies (GISS) climate model (Hansen *et al* 1983). Its radiation scheme includes all significant greenhouse gases and 11 types of aerosols. The model of atmospheric chemistry represents climate-relevant reactive trace-gases and aerosols and includes: convergent and convective transports; parameterized north–south eddy transport; local true production or loss due to surface emission or deposition; and atmospheric chemical reactions (Wang *et al* 1998). The Community Land Model (CLM) version 3.5 (Oleson *et al* 2008) is implemented as the IGSM land-surface scheme. CLM explicitly treats thermal and hydrologic frozen soil and freeze/thaw processes as well as snow processes. The IGSM consistently depicts the global and zonal profiles of present-day climate and potential climate change when compared with observations (Sokolov and Stone 1998) and the Intergovernmental Panel on Climate Change (IPCC) Fourth Assessment Report (AR4) archive (Sokolov *et al* 2009, Schlosser *et al* 2013), respectively.

We assess the present-day near-surface permafrost and climate change-induced degradation by forcing CLM off-line with atmospheric data obtained from the IGSM fully coupled transient 20th and 21st century climate change integration (Sokolov *et al* 2009). The IGSM is forced from 1861 to 1990 by observed changes in greenhouse gas (GHG) concentrations and from 1991 forward by emissions of GHG and aerosol precursors projected by the EPPA model (Sokolov *et al* 2009). The suite of model simulations encompasses the range in emission pathways (Unconstrained Emission (UCE) and Greenhouse gas Stabilization (GST) emission scenarios) as well as the large-scale transient climate response (TCR) that aggregates the effect of three key climate parameters (climate sensitivity, ocean heat uptake rate, and net aerosol forcing) (table 1). We attempt to assess uncertainty in our projections resulting from the climate response as well as from emissions. As such, climate-parameter values and emission rates are chosen in combination to produce the high (95%), median (50%), and low (5%) percentiles of the probability distributions of surface-air temperature increase from a 400-member ensemble simulation. Projected unconstrained anthropogenic emissions are quite sensitive to the choice of uncertain economic model parameters (such as population growth, labor productivity, etc), therefore

the three different levels of emission rates are considered for the UCE scenario. Conversely, the GST emission scenarios are heavily constrained to meet a stabilization target and thus have very similar emission pathways (although the cost of achieving these stabilizations differ). Therefore only the median-emission pathway is considered for the GST scenario. Overall, the median UCE and GST emission scenarios here are roughly equivalent to the IPCC's Representative Concentration Pathways 8.5 and 4.5, respectively. A downscaling technique (Schlosser *et al* 2013) expands the IGSM zonal near-surface meteorology to generate corresponding longitudinal patterns (supplementary materials available at stacks.iop.org/ERL/8/035014/mmedia). The climatology of these patterns is derived from observations and the resulting geographic fields compare favorably with the observations (supplementary figures 1, 2 available at stacks.iop.org/ERL/8/035014/mmedia). Pattern shifts in response to human-forced change are also applied for 21st century climate change based on climate-model results from the IPCC AR4 archive (Schlosser *et al* 2013). As such, the uncertainty in regional climate change characterized by each IPCC AR4 participating climate model can be considered. With these forcing fields, a set of CLM simulations (table 1) has been conducted at a 2° × 2.5° resolution through the 21st century.

With regard to modeling the landscape, CLM, like any land-surface scheme, coupled within earth-system models, does not explicitly track surface subsidence induced by ice-rich permafrost thaw. These thermokarst landforms occur at spatial scales well below those resolved in regional and global models, and so the surface water retention—if any—that directly results from this (thermokarst) process would be underrepresented and the resulting methane emissions be underestimated. The extent to which these fine-scale processes support a climate-warming feedback at the regional scale will be addressed in our sensitivity analysis. Nevertheless, our model framework captures large-scale hydro-climate processes (i.e. precipitation, evaporation, sub-surface soil physics) that are highly relevant to large-scale saturated-area expansion, methane emissions, and resulting radiative forcing. Our intent here is not to provide a deterministic prediction of permafrost thaw and inundation, but rather to examine through an integrated assessment model framework the temperature feedback from a range of plausible CH_4 emission responses that could occur as a result of human-induced climate warming and to examine a threshold of methane-emission increase for such temperature feedback to be salient. We assume any modeled inundation of thawed permafrost regions takes the form of wetlands and lakes. Using this simplified land-surface modeling approach coupled to an earth-system model (i.e. the IGSM), we are able to determine what threshold of methane-emission increase would result in a salient positive climate-warming feedback.

3. Results and discussion

Each model grid, having a 3.5 m soil-column depth, is identified as containing permafrost if monthly soil temperature in at least one sub-surface soil layer remains at or below 0 °C for two or more consecutive years. Delisle (2007) argued the likely overestimates of permafrost degradation with a 3.5 m soil-column depth. Lawrence *et al* (2008) found that the rate of near-surface permafrost loss is not strongly affected by inclusion of the deep thermal reservoir associated with new soil layers. In our CLM simulations, the near-surface permafrost area, poleward of 45°N and excluding glacial regions, is 11.2 × 10^6 km^2 averaged from 1970 to 1989 (annual values vary from 10.9 to 11.5 × 10^6 km^2 during that period) with median TCR and emission parameters. The result falls on the lower bound of the observationally based range of continuous and discontinuous permafrost extent (11.2 to 13.5 × 10^6 km^2) over the same period (Zhang *et al* 2000). The lack of subgrid soil-column representation may prevent the explicit simulation of the sporadic or isolated permafrost categories, and thus contribute to our lower extent. Through the 21st century, the simulations indicate a nearly linear near-surface permafrost degradation rate, with the potential for 75% loss for the low TCR and nearly 100% loss for the high TCR cases by 2100 under a median-emission UCE scenario (figure 1). We also find that uncertainties in emissions (dotted lines) are as important as climate-response uncertainty (thick solid lines), in terms of contributing to the total uncertainty in projected permafrost changes. Under a GST scenario of 560 ppm CO_2-equivalent concentration by 2100, permafrost degradation reduces substantially, with 20% loss for low TCR and 40% loss for high TCR by 2100. In addition, uncertain regional climate change (figure 1, light thin lines) may accelerate the permafrost thaw by 5%–10% due to enhanced warming over land imposed by the climate-model patterns.

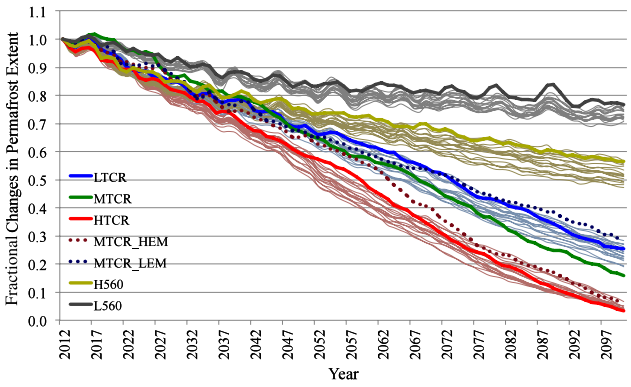

Figure 1. Fractional change in near-surface permafrost extent (poleward of 45°N and in a nonglacier area) with respect to 2012 (around 1.02 × 10^{13} m^2) under various climate projections. Thick lines represent the use of climatological geographic patterns in near-surface meteorology throughout the 21st century. Light thin lines represent the inclusion of additional geographic pattern shifts from the IPCC AR4 climate-model projections. The figure legend is detailed in table 1.

Next we estimate the potential methane-emission increase. In areas of permafrost, ground water level is greatly influenced by the existence of the underlying impervious permafrost layer. Surface infiltration and water released by the melting of frozen soil supply water to the thawed zone above the permafrost layer. Unless the soil is relatively pervious and

the terrain has sufficient slope to permit lateral drainage, the water table may rise to, or near, the ground surface. We draw from previous work (Koven *et al* 2011, Gedney *et al* 2004) and interpret the model's diagnoses of land area where the water table has reached the ground surface (or 'saturated land area') as a concurrent CH_4-emitting area. The calculation of 'saturated soil fraction' in CLM explicitly accounts for the aforementioned major hydrologic and topographic controls of water table variations for an unconfined aquifer. To confirm that our simulated saturated land area is a reasonable proxy of inundated area, important to control large-scale CH_4 emission, we compared the simulation with the 1993–2007 global inundated areas inferred from multiple satellite observations (Prigent *et al* 2007). Satellite observations capture, but do not discriminate among, inundated wetlands, rivers, and small lakes. CLM-simulated saturated areas also do not make these distinctions. Further, both estimates will not capture localized inundated areas—yet as we will show in a sensitivity analysis, these localized effects will require orders of magnitude larger emissions to impact the global temperature biogeochemical feedback response considered herein. Despite these considerations, satellite reconstruction provides a first-order estimate of global inundation (Prigent *et al* 2007). Our simulated saturated areas are mostly consistent with the temporal patterns of the satellite reconstruction at large spatial scales (supplementary figure 3 available at stacks.iop.org/ERL/8/035014/mmedia). Over the region of our interest (poleward of 45°N), the simulations agree within ∼1% of the satellite estimate with the 15-year annual means of 8.00×10^5, 7.93×10^5, and 8.00×10^5 km^2 under low, median, and high TCR with median-emission parameters against the observation of 8.04×10^5 km^2. In terms of expansion of CH_4-emitting areas across the 21st century scenarios, the model-predicted saturated area integrated north of 45°N increases 15%–25% by 2100 for the low and high TCR, respectively, under the median-emission UCE scenario (figure 2). Under the GST scenario, the expansion of saturated areas is limited to 5% and 15% for the low and high TCR, respectively. Uncertain regional climate changes can enhance saturated-area expansion, especially for the high TCR of the UCE scenario, to as much as 30%–50% by 2100 (thin red lines). Overall, the total estimated saturated area increases from 5% to 50% by 2100 across all the projections.

For CH_4 emission estimates, we interpret our inferred total saturated area (hereinafter inundated area) into two types of CH_4-emitting surfaces: wetlands and lakes. We assumed a wetland:lake ratio of 3.35 (77% versus 23% coverage, respectively) based on the occurrences of these wet surface types north of 45°N in the Global Lakes and Wetlands Database (GLWD) (Lehner and Döll 2004). Alternative interpretations of the inferred total inundated area (as wetlands or lakes only) show little effect on the resulting CH_4 emission estimates (provided below). We further account for a key distinction for lakes: yedoma versus non-yedoma based on a contemporary atlas of yedoma regions. Yedoma regions are underlain by ice-rich, organic-rich Pleistocene-age soil (Zimov *et al* 1997), and measurements taken at yedoma lakes show significantly

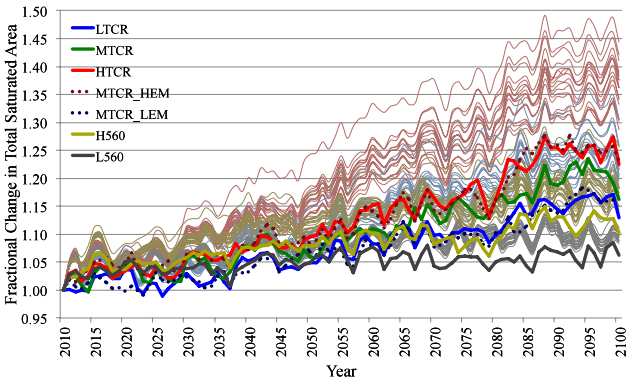

Figure 2. Fractional change in the total saturated area (poleward of 45°N and excluding glacier) with respect to 2010 (around 8.1×10^{11} m^2) under various climate projections.

higher ebullition CH_4 fluxes (139 g-CH_4 m^{-2} yr^{-1}) than non-yedoma counterparts (5.9 g-CH_4 m^{-2} yr^{-1}) (Walter *et al* 2006, 2012). In each grid cell, CH_4 emissions are calculated independently for each CH_4-emitting surface type and then aggregated. Additionally, we model the temperature regulation of methanogenesis in each surface type using a Q_{10} relationship (supplementary materials available at stacks.iop.org/ERL/8/035014/mmedia). We estimate a CH_4 emission of 21 Tg-CH_4 yr^{-1} from lakes and wetlands poleward of 45°N at 2010. This, combined with additional 25 Tg-CH_4 yr^{-1} from northern bogs (Schlosser *et al* 2007), falls within the range (20–72 Tg-CH_4 yr^{-1}) of a comprehensive assessment of CH_4 emissions for northern regions from top-down and bottom-up techniques (EPA 2010). By the end of the 21st century, under the UCE scenario, increases in decadal averaged (2091–100) annual CH_4 emission from inundated area expansion and Q_{10} warming range between 5.6–8.9 Tg-CH_4 yr^{-1} and 9.7–15.1 Tg-CH_4 yr^{-1} for the low and high TCR cases, respectively, of which approximately 80% is contributed by wetlands and 20% by lake (figure 3). This is mostly associated with the larger percentage of inundated area we specify for wetlands. Nevertheless, these increases, which are at most 75% of the 2010 estimate from lakes and wetlands, are considerably lower than the IGSM estimated human global CH_4 emission increase of 349 Tg-CH_4 yr^{-1} over the same period (supplementary figure 4 available at stacks.iop.org/ERL/8/035014/mmedia). Under the GST scenario, the CH_4 emission increases by 2100 are substantially lower relative to the UCE scenario. The decadal averaged annual emission increases are 0.8–1.7 Tg-CH_4 yr^{-1} and 2.3–4.1 Tg-CH_4 yr^{-1} for the low and high TCR cases, respectively. However, unlike the UCE scenario, these increases are quite comparable to the corresponding IGSM estimated global CH_4 human-emission increase at 4 Tg-CH_4 yr^{-1} through the 21st century (supplementary figure 4). Across all the modeled scenarios, about 52–58% of these aforementioned emission increases are a result of warming pre-existing inundated areas with the remaining increases due to newly formed inundated areas from permafrost thaw.

To assess the potential climate-warming feedback from these increases in CH_4 emissions, we then integrate the fully

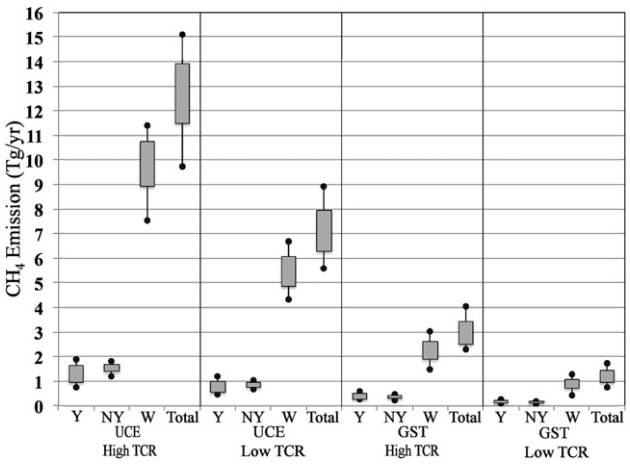

Figure 3. Increases in decadal averaged (2091–2100) annual CH_4 emission ($Tgyr^{-1}$, poleward of 45°N) with respect to 2011–20 as a result of the warming and expansion of yedoma lakes (Y), non-yedoma (NY) lakes, wetlands (W), and total inundated areas for the low and high TCR under the UCE and GST scenarios, respectively. Each scenario contains 18 ensemble members (17 members of model-based pattern shifts and one member of climatological pattern). Whisker plots show the minimum, maximum, and plus/minus one standard deviation about the ensemble mean.

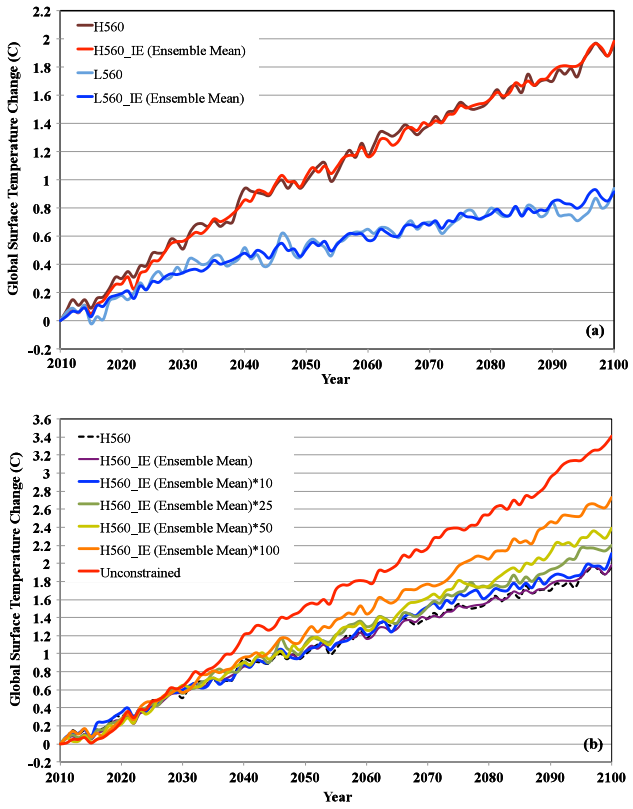

Figure 4. (a) Global temperature change from increased CH_4 emission due to the warming and expansion of thawed, inundated areas for the low and high TCR of the GST scenario. IE refers to the CH_4 inundation emission. (b) The sensitivity of global temperature change (°C) to the increased CH_4 inundation emission for the high TCR of the GST scenario. 10, 25, 50, and 100 refer to the CH_4 inundation emission increases scaled by 10-, 25-, 50-, and 100-fold, respectively. Also shown is the global temperature change with the UCE scenario.

coupled IGSM and exogenously prescribe the corresponding CH_4 emission increases through the 21st century. With the full capacity of IGSM's atmospheric chemistry, the assessment of such feedback is coupled within the atmospheric methane cycle to account for the change in the balance of atmospheric methane oxidation rates, methane lifetime and concentration as a result of increased methane emission. For the UCE scenario, the ensemble-mean result shows no discernable temperature feedback as the increases in anthropogenic emissions overwhelm the emission response from inundated area warming and expansion (not shown). For the ensemble-mean GST scenario, no salient global temperature feedback is discernable for either the high or the low TCR case in response to the added CH_4 emission (figure 4(a)). Among all the simulations performed (table 1), only one member of the GST scenario ensemble, which accounts for uncertain regional climate changes, exhibits a small temperature feedback of approximately 0.1°C towards the end of this century, although this warming is somewhat overshadowed by interannual variability. Although the range of the end-of-century increase in CH_4 emission (0.8–4.1 Tg-CH_4 yr^{-1}) is comparable to the human-induced CH_4 emission increase (4 Tg-CH_4 yr^{-1}) under the GST scenario, it is still quite low (on the order of 1%) when compared with the current level of human CH_4 emission rates (∼345 Tg-CH_4 yr^{-1} at 2010, supplementary figure 4), and particularly when considering all greenhouse gas emissions. Further IGSM tests indicate that a 1% CH_4 emission increase has a very minor effect on radiative forcing (supplementary figure 5 available at stacks.iop.org/ERL/8/035014/mmedia).

Given the uncertainty in our CH_4 emission estimates caused by parameter uncertainty as well as the aforementioned model limitations, we attempt to characterize the relative strength of the derived CH_4 emission response, particularly with respect to additional CH_4 emissions needed to achieve a salient climate-warming feedback. We perform sensitivity experiments by augmenting the CH_4 emissions and repeating the 21st century IGSM projections. Each run separately considers: scaling the aforementioned estimated CH_4 emission increases by 10-, 25-, 50-, and 100-fold; as well as applying the UCE scenario. Results for the GST scenario at the high TCR are examined. We find that the 10-fold increase would not support a salient temperature-feedback response (figure 4(b)). The 100-fold increase produces a temperature response of about 0.8 °C by 2100, but salient only after mid-century. The UCE scenario causes temperature to rise ∼1.5 °C by 2100. At a 25-fold emission increase, a discernable, additional warming of 0.2 °C is evident only in the last decade of the 21st century.

Overall, these results cast a quantitative insight on the strength and range of the global climate-warming biogeochemical feedback from near-surface permafrost thaw and subsequent CH_4 emission. This model-based investigation is the first of its kind in its use of an integrated assessment model to systematically account for key sources of uncertainty stemming from human-emission

pathways, global climate sensitivity, and regional climate change shifts. The increase in CH_4 emission due to potential Arctic/boreal thawed, inundated area warming and expansion represents a weak climate-warming feedback within this century. This is consistent with previous studies (Anisimov 2007, Huissteden *et al* 2011, Delisle 2007) that also imply a small Arctic lake/wetland biogeochemical climate-warming feedback. Riley *et al* (2011) discussed many deficiencies and uncertainties that currently exist in modeling methane production and emission—most of them are also applicable for this study. Fundamental processes resulting in small-scale inundation (e.g. thermokarst lake dynamics) are lacking here—such landforms have been shown to increase rapidly and may have a large impact on CH_4 fluxes (Turetsky *et al* 2007). Further, buffering effects from lake drainage are not explicitly considered, however these drainage effects would further weaken the already small feedback found (Huissteden *et al* 2011, Avis *et al* 2011). Further uncertainty arises from: the simulated grid fractional saturation that is of first-order importance to CH_4 emission estimates; spatially heterogeneous field-based CH_4 emission flux; parameters associated with the temperature dependence of CH_4 production; and a possible increase of geological and hydrate emissions (particularly in areas underlain by relatively thin permafrost). Although the satellite reconstruction provides a good estimate of global inundation, it is inadequate in characterizing small, isolated water bodies, including some of those formed by the thermokarst process. Other factors that could be important but not explicitly considered include: the insulating peat (Lawrence *et al* 2008) and fire disturbance for permafrost thaw as well as soil-moisture and vegetation dynamics, and methane oxidation removal processes ongoing in soils, sediments, and water. However, many of these factors may serve as buffering effects on the CH_4 emission response, and small feedback as well. Nevertheless, among these aforementioned considerations that could enhance CH_4 emission response, an order of 25-fold increase to our modeled response would be required to change our overall conclusion: the biogeochemical global climate-warming feedback from increased CH_4 emissions due to thawed, inundated area warming and expansion is relatively small, whether or not humans choose to constrain global emissions.

Acknowledgment

The authors gratefully acknowledge the Department of Energy Climate Change Prediction Program Grant DE-PS02-08ER08-05 and Office of Science (Biological and Environmental Research) US Department of Energy in supporting this work.

References

Alexeev V A, Nicolsky D J, Romanovsky V E and Lawrence D M 2007 An evaluation of deep soil configurations in the CLM3 for improved representation of permafrost *Geophys. Res. Lett.* **34** L09502

Avis C A, Weaver A J and Meissner K J 2011 Reduction in areal extent of high-latitude wetlands in response to permafrost thaw *Nature Geosci.* **4** 444–8

Anisimov O A 2007 Potential feedback of thawing permafrost to the global climate system through methane emission *Environ. Res. Lett.* **2** 045016

Bastviken D, Tranvik L J, Downing J A, Crill P M and Enrich-Prast A 2011 Freshwater methane emission offset the continental carbon sink *Science* **331** 50

Christensen T R, Johansson T, Akerman H J, Mastepanov M, Malmer N, Friborg T, Crill P and Svensson B H 2004 Thawing sub-arctic permafrost: effects on vegetation and methane emissions *Geophys. Res. Lett.* **31** L04501

Delisle G 2007 Near-surface permafrost degradation—how severe during the 21st century? *Geophys. Res. Lett.* **34** L09503

EPA (Environmental Protection Agency) 2010 Methane and nitrous oxide emissions from natural sources *EPA 430-R-10-001* (Washington, DC: US Environmental Protection Agency)

Gedney N, Cox P M and Huntingford C 2004 Climate feedback from wetland methane emissions *Geophys. Res. Lett.* **31** L20503

Hansen J, Russell G, Rind D, Stone P, Lacis A, Lebedeff S, Ruedy R and Travis L 1983 Efficient three-dimensional global models for climate studies: models I and II *Mon. Weather Rev.* **111** 609–62

Huissteden J V, Berrittella C, Parmentier F J W, Mi Y, Maximov T C and Dolman A J 2011 Methane emissions from permafrost thaw lakes limited by lake drainage *Nature Climate Change* **1** 119–23

Koven C D, Ringeval B, Friedlingstein P, Ciais P, Cadule P, Khvorostyanov D, Krinner G and Tarnocai C 2011 Permafrost carbon-climate feedbacks accelerate global warming *Proc. Natl Acad. Sci. USA* **108** 14769–74

Lawrence D M, Slater A, Romanovsky V E and Nicolsky D J 2008 Sensitivity of a model projection of near-surface permafrost degradation to soil column depth and representation of soil organic matter *J. Geophys. Res.* **113** F02011

Lawrence D M and Slater A G 2005 A projection of severe near-surface permafrost degradation during the 21st century *Geophys. Res. Lett.* **32** L24401

Lehner B and Döll P 2004 Development and validation of a global database of lakes, reservoirs and wetlands *J. Hydrology* **296** 1–22

Oleson K W, Niu G Y, Yang Z L, Lawrence D M, Thornton P E, Lawrence P J, Stöckli R, Dickinson R E, Bonan G B and Levis S 2008 Improvements to the community land model and their impact on the hydrological cycle *J. Geophys. Res.* **113** G01021

Prigent C, Papa F, Aires F, Rossow W B and Matthews E 2007 Global inundation dynamics inferred from multiple satellite observations, 1993–2000 *J. Geophys. Res.* **112** D12107

Riley W J, Subin Z M, Lawrence D M, Swenson S C, Torn M S, Meng L, Mahowald N M and Hess P 2011 Barriers to predicting changes in global terrestrial methane fluxes: analyses using CLM4Me, a methane biogeochemistry model integrated in CESM *Biogeosciences* **8** 1925–53

Schlosser C A, Gao X, Strzepek K, Sokolov A, Forest C, Awadalla S, Farmer W and Jacoby H 2013 Quantifying the likelihood of regional climate change: a hybridized approach *J. Clim.* **26** 3394–414

Schlosser C A, Kicklighter D and Sokolov A 2007 Global land system framework for integrated climate-change assessments *MIT Joint Program on the Science and Policy of Global Change Report* vol 147

Schuur E A G and Abbott B 2011 Climate change: high risk of permafrost thaw *Nature* **480** 32–3

Shindell D, Walter B P and Faluvegi G 2004 Impacts of climate change on methane emissions from wetlands *Geophys. Res. Lett.* **31** L21202

Smith L C, Sheng Y, MacDonald G M and Hinzman L D 2005 Disappearing Arctic lakes *Science* **308** 1429

Sokolov A P and Stone P H 1998 A flexible climate model for use in integrated assessments *Clim. Dyn.* **14** 291–303

Sokolov A P, Stone P H, Forest C E, Prinn R, Sarofim M C, Webster M, Saltsev S and Schlosser C A 2009 Probabilistic forecast for twenty-first-century climate based on uncertainties in Emissions and climate parameters *J. Clim.* **22** 5175–204

Sokolov A P *et al* 2005 The MIT Integrated Global System Model (IGSM) Version 2: Model description and baseline evaluation *MIT Joint Program on the Science and Policy of Global Change Report* vol 124

Turetsky M, Weider R K, Vitt D H, Evans R J and Scott K D 2007 The disappearance of relict permafrost in boreal North America: effects on peatland carbon storage and fluxes *Glob. Change Biol.* **13** 1922–34

Walter K M, Anthony P, Grosse G and Chanton J 2012 Geologic methane seeps along boundaries of arctic permafrost thaw and melting glaciers *Nature Geosci.* **5** 419–26

Walter K M, Zimov S A, Chanton J P, Verbyla D and Chapin F S III 2006 Methane bubbling from Siberian thaw lakes as positive feedback to climate warming *Nature* **443** 71–5

Wang C, Prinn R G and Sokolov A 1998 A global interactive chemistry and climate model: formulation and testing *J. Geophys. Res.* **103** 3399–418

Zhang T, Heginbottom J A, Barry R G and Brown J 2000 Further statistics on the distribution of permafrost and ground-ice in the Northern Hemisphere *Polar. Geogr.* **24** 126–31

Zimov S A, Voropaev Y V, Semiletov I P, Davidov S P, Prosiannikov S F, Chapin F S, Chapin M C, Trumbore S and Tyler S 1997 North Siberian lakes: a methane source fuelled by Pleistocene carbon *Science* **277** 800–2